KARYA ILHAM PUBLISHING
CONNECTING MINDS, BRIDGING IDEAS, INSPIRING READERS

Advances in Fluid, Heat and Materials Engineering

Journal homepage:
https://karyailham.com.my/index.php/afhme/index
ISSN: 3083-8134

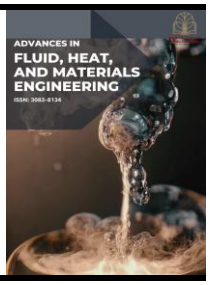

Simulation of Internal Flow Behaviour on the Different Diameter of Y-Junction Pipe

Muhammad Dzul Imran Ismail[1,*]

[1] Faculty of Mechanical Engineering and Manufacturing, Universiti Tun Hussien Onn Malaysia, 86400 Parit Raja, Johor, Malaysia

ARTICLE INFO

Article history:
Received 15 June 2025
Received in revised form 29 July 2025
Accepted 5 August 2025
Available online 29 September 2025

Keywords:
Y-junction pipe; computational fluid dynamics; pressure and velocity distribution

ABSTRACT

Pipelines are widely used in many industries for transporting water, chemicals, and other fluids, and their performance is strongly influenced by the behaviour of the fluid inside them. When a Y-junction is included in the pipeline, the flow is often affected by uneven speed, increased turbulence, and pressure losses. Although several studies have been conducted on flow in junctions, limited attention has been given to how pipe size and flow speed together influence the behaviour inside a Y-junction. In this study, this gap was addressed by examining how different pipe diameters and inlet velocities affect internal flow patterns. Computer simulations were carried out using ANSYS Fluent, where two pipe diameters (0.1 m and 0.2 m) and three inlet velocities (0.297 m/s, 0.397 m/s, and 0.497 m/s) were tested. From the results, it was observed that smaller pipes caused higher flow speed, greater turbulence, and a sharper pressure drop. In contrast, larger pipes produced slower and more stable flow with smoother pressure distribution. Through this analysis, useful insights were provided for improving the design of Y-junction pipelines, where better flow stability, reduced energy loss, and higher system efficiency can be achieved.

1. Introduction

Internal pipeline flow is a fundamental component of fluid transmission systems, widely used across various engineering fields such as water distribution, heat exchangers, and chemical processing [1,2]. Understanding the complex flow behavior, particularly in turbulent conditions, is crucial for optimizing system performance and preventing failures [1,3]. While flow in straight pipes is well-understood, the introduction of junctions, such as the Y-junction, creates intricate flow patterns characterized by secondary flows, flow separation, and vortex formation [4-7]. The geometry of these junctions, specifically the angle between branches, profoundly affects the resulting velocity and pressure distributions [8]. Furthermore, fluid dynamics at junctions can lead to elaborate flow regimes that can trap particles, a key consideration in the proper functioning of piping networks [9].

* *Corresponding author.*
E-mail address: CD210013@student.uthm.edu.my

https://doi.org/10.37934/afhme.6.1.5062a

Given the challenges and high costs associated with physical experimentation, Computational Fluid Dynamics (CFD) has become an invaluable tool for visualizing and analyzing flow behavior in complex geometries [1,2,10]. CFD simulations allow engineers to test a wide range of conditions without the need for extensive physical testing [11]. Previous studies have used CFD to explore the effects of junction geometry on mixing efficiency and hydraulic short circuits [4,12-14]. Recent developments in CFD tools have also enabled more accurate prediction of erosion and mechanical stresses, which helps in designing more durable piping systems [15]. However, accurate predictions require careful consideration of turbulence models and refined meshing, especially in areas with high flow gradients [1,16]. The significance of validating CFD results against experimental data is also a well-established practice to ensure the reliability of computational models [10,17,18].

Although prior research has investigated various aspects of branched pipe flows, there is a lack of detailed, comparative studies that systematically analyze the combined effects of both pipe diameter and flow rate on the internal flow characteristics of a Y-junction. This paper addresses this gap by employing sophisticated CFD methods to simulate and analyze the flow features within a Y-junction pipe. The study specifically examines the influence of two different pipe diameters (0.1 m and 0.2 m) and three inlet velocities (0.297 m/s, 0.397 m/s, and 0.497 m/s) on key properties: velocity distribution, static pressure, and turbulence kinetic energy. The findings from this research will provide a valuable reference for the optimal design of Y-junction pipelines and for predicting flow performance in engineering systems [19,20]. The results will help guide design decisions to avoid issues like imbalanced flow distribution and high-pressure loss [6,11].

2. Methodology

2.1 Geometry Construction

In this study, two computational models representing straight pipe sections were developed to analyse internal flow dynamics using CFD. The first model (Diameter 1) had a length of 1.0 m and a diameter of 0.1 m, while the second model (Diameter 2) also had a length of 1.0 m but with a larger diameter of 0.2 m as shown in Figure 1. These geometries were designed using ANSYS Design Modeler to ensure accurate representation of the pipe flow domain. The aim was to observe how variations in pipe diameter influence velocity, pressure, and turbulence characteristics under identical inlet conditions. The geometry was kept simple, with no branching or bends, to isolate the effects of diameter alone.

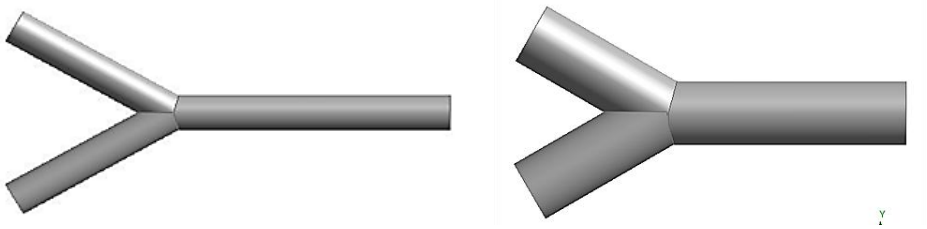

(a) (b)

Fig. 1. Diameter of geometry pipeline (a) 0.1 m (b) 0.2 m

2.2 Mesh Generation and Grid Independent Test

The meshing process was carried out using ANSYS Meshing, employing a structured tetrahedral mesh with inflation layers applied near the wall surfaces to capture boundary layer effects more accurately. To ensure mesh independence, three different element sizes were tested: 0.02 m (Mesh 1), 0.019 m (Mesh 2), and 0.018 m (Mesh 3), as shown in Table 1. Simulation results, including velocity

and pressure distribution, were compared across these three mesh cases. The comparison showed that the results between Mesh 2 and Mesh 3 were nearly identical, indicating that further mesh refinement beyond 0.019 m did not yield significant accuracy improvements. Hence, Mesh 2 was selected for all final simulations as it provided a good balance between accuracy and computational efficiency.

Table 1
Grid independence test (GIT)

Diameter (m)	Element size (m)
0.01	0.02
	0.019
	0.018
0.02	0.02
	0.019
	0.018

2.3 Boundary Condition and Flow Parameter

The simulations were conducted under turbulent flow conditions for water at room temperature (Tables 2 and 3). At the inlet, three different uniform velocity values were applied: 0.297 m/s, 0.397 m/s, and 0.497 m/s. These inlet velocities were tested for both pipe diameter models to assess the combined impact of velocity and diameter on internal flow behaviour. The outlets were set as pressure outlets with zero-gauge pressure, while the pipe walls were defined as no-slip boundaries. The working fluid was assumed incompressible with constant density and viscosity. The standard k-ε turbulence model was selected due to its reliability and widespread application in internal pipe flow simulations.

Table 2
Boundary condition of straight line

Boundary Type	Location	Condition type	Value
Inlet	Pipe entrance	Velocity inlet	0.297 m/s, 0.397 m/s, 0.497 m/s
Outlet	Pipe exit	Pressure outlet	0 Pa (gauge pressure)
Wall	Pipe inner wall	No-slip wall	Velocity = 0 m/s at the surface

Table 3
Turbulent flow conditions

Diameter (m)	Velocity 1 m^{s-1}	Velocity 2 m^{s-1}	Velocity 3 m^{s-1}	Outlet	Turbulence intensity	Turbulence model
0.1	0.297	0.397	0.497	0	5%	$k-\omega$
0.2	0.297	0.397	0.497	0	5%	$k-\omega$

2.4 Post-Processing and Flow Analysis Parameters

Post-processing was carried out using ANSYS Fluent to analyse the internal flow characteristics. Key parameters extracted included velocity magnitude, turbulence kinetic energy (TKE), and pressure. Contour plots, vector flow diagrams, and line graphs were generated to visualize the flow development and identify changes in flow behaviour due to variations in diameter and inlet velocity.

Additionally, cross-sectional profiles were used to examine the uniformity of flow and detect any signs of secondary motion or recirculation zones.

3. Results

3.1 Grid Independent Test

The meshing process was carried out using ANSYS Meshing, employing a structured tetrahedral mesh with inflation layers applied near the wall surfaces to capture boundary layer effects more accurately. To ensure mesh independence, three different element sizes were tested: 0.02 m (Mesh 1), 0.019 m (Mesh 2), and 0.018 m (Mesh 3), as shown in Table 4. Simulation results, including velocity and pressure distribution, were compared across these three mesh cases. The comparison showed that the results between Mesh 2 and Mesh 3 were nearly identical, indicating that further mesh refinement beyond 0.019 m did not yield significant accuracy improvements. Hence, Mesh 2 was selected for all final simulations as it provided a good balance between accuracy and computational efficiency, as shown in Figure 2.

Table 4
Value of element sizing

Diameter (m)	Element size (m)	Nodes
0.01	0.02	22504
	0.019	26629
	0.018	31074
0.02	0.02	81928
	0.019	95089
	0.018	111102

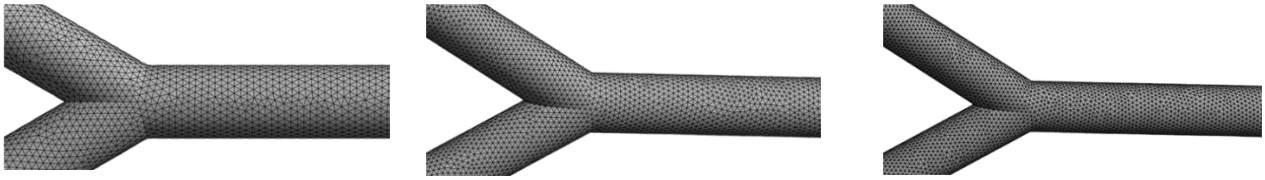

(a) (b) (c)

Fig. 2. Meshing (a) 0.02 (b) 0.019 (c) 0.018

In the current study, it is chosen to consider two different pipe diameters 0.1 meters and 0.2 meters. In each case, three different mesh densities are defined by changing the value of “element sizing” which, in essence, defines how fine or how coarse the mesh can be. For the 0.1 m diameter pipe, as shown in Table 1, the largest, essentially coarsest mesh with the element sizing 0.02 m, results in 22,504 elements. With the binary decrease to 0.019 and 0.018, the number of elements grows to 26,629 and 31,074, respectively. Such growth occurs because the existence of more elements allows simulation to more fully grasp the changes that take place during the flow, especially near the walls and near the intersections when most changes take place. For the 0.2 m diameter pipe, as shown in Table 3, the trends are similar but occur on a larger scale.

Thus, at the largest element size of 0.02, there are 81,928 elements, and at the smallest of 0.018 m, there is a 111,102-element mesh. More elements are needed because the greater size of a pipe refers to more volume and more outer surfaces that need to be covered, which requires more elements to make the mesh similar in detail. The pictures under the tables are provided to compare the visual image of the Y-junction pipe under different mesh densities. Image A corresponds to the largest element size of 0.02 m and, thus, the coarsest mesh, with a distinct structure of the elements.

Image B corresponds to 0.019 m and already shows a denser mesh, through a thorough proportion of the pipe dimensions.

Finally, Image C corresponds to the element size of 0.018 m and shows very dense and structured mesh that fills most parts of the pipe. To summarize, these tables and images provide the argument for the refinement of the mesh. Fibrous reduction in the element size makes the mesh more detailed to ensure the higher level of the CFD simulation accuracy. Nonetheless, this directly increases the computational requirement because more elements equal more calculations for the computer. The CFD choice to lower the element size should always balance between higher quality and effort a crucial balance in any CFD study.

For the 0.1 m diameter pipe, you are starting just above 0.5 m/s at the inlet. As the fluid proceeds down the pipe, the velocity ramps up rapidly in the first 0.2 m (Figure 3). Beyond that initial climb, the rise levels off and the velocity approaches a constant value, about 0.66m per second, at the far end of the pipe. This pattern indicates the fluid initially accelerates rapidly and then enters into a steady flow as it moves downstream. Similarly, the 0.2 m pipe shows the same trend, with a few distinctions. The initial speed is also slightly higher, just above 0.5 m/s, but the rate of acceleration is a bit less dramatic. The fluid stops accelerating after a while, and stabilizes at about 0.62 m/s. It is an indication that faster stabilization is attained for the wider pipe; however, the maximum velocity is a bit smaller compared to the narrower pipe.

In general, these findings demonstrate the impact of the pipe diameter on the fluid velocity evolution. In either case the flow becomes more stable and uniform further downstream of the entrance, but the narrower pipe permits a higher flow speed at the end and the wider pipe stabilizes the flow sooner.

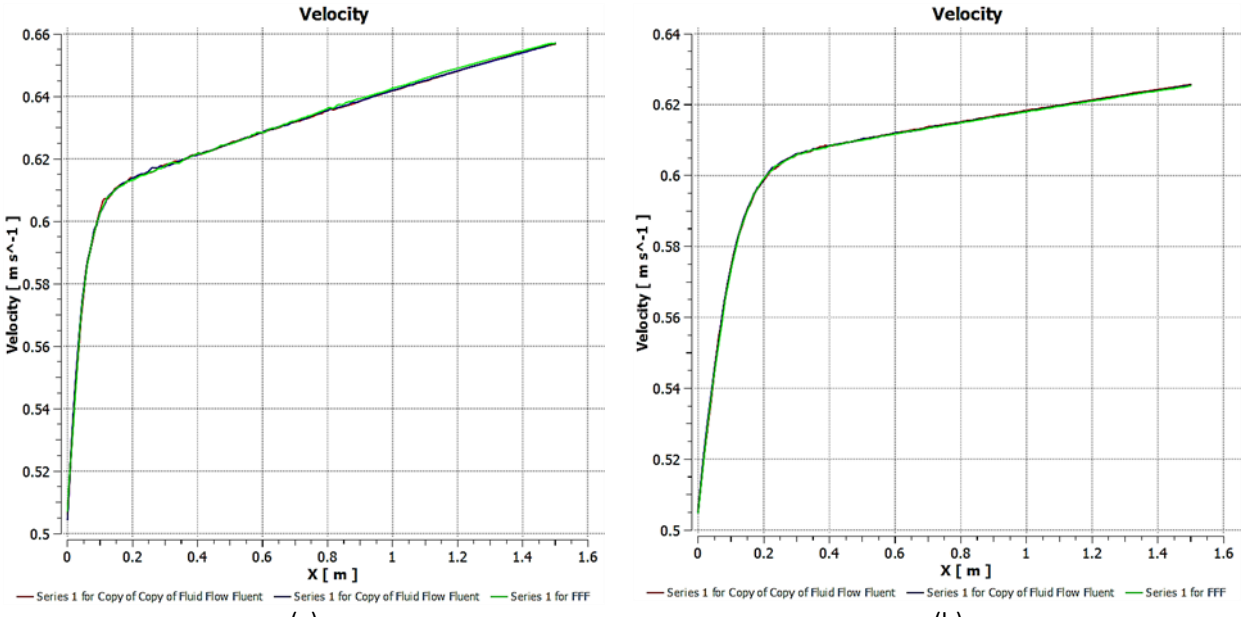

(a) (b)

Fig. 3. Graft quality of velocity vs X (a) Diameter 0.01 m (b) Diameter 0.02 m

For the narrower tube (0.1 meter in diameter) the value of the turbulent kinetic energy at the first-time step is quite high, ranging between 0.00035 m^2/s^2 to 0.0004 m^2/s^2 near the pipe inlet, shown in Figure 4. In the early region, the curves of the two numbers for the three different simulations or measurement series exhibit small fluctuations small jumps and small decreases which means the turbulence has not yet decayed to a state where it is adapted to the geometry of the pipe. Turbulent energy also starts decreasing after the first 0.1 m to 0.2 m down the pipe. At around

the meter scale, the turbulence has decayed significantly, dropping to values of around 0.0001 m^2/s^2. This means that the chaotic motion of the fluid is relaxing toward calm as it moves away from the entrance, arriving at a more ordered state.

In the larger 0.2 m diameter pipe, we observe a comparable pattern, although with some slight differences. The initial turbulent kinetic energy is only a bit smaller, slightly below 0.0002 m^2/s^2. On the narrower pipe, there are also some ripples further back in the chart, but not so pronounced. With the advancing flow the decay of turbulence is less abrupt and complete as is evident by the convergence of all three curves as flow evolves. The energy of this turbulence has again mostly dissipated and by the time the fluid has travelled to the other end of the pipe the turbulent energy is almost as low as that of the smaller pipe.

What the charts here tell us, that turbulence is maximized at the spot where the fluid enters the pipe, especially in the narrower pipe where energy and the chaos are heightened. As the liquid moves further through the tube, the turbulence naturally diminishes and the flow seems calmer and more regular. The fatter pipe appears to make the fluid quiet down slightly more rapidly with initially less violent and a smoother progression to steady flow.

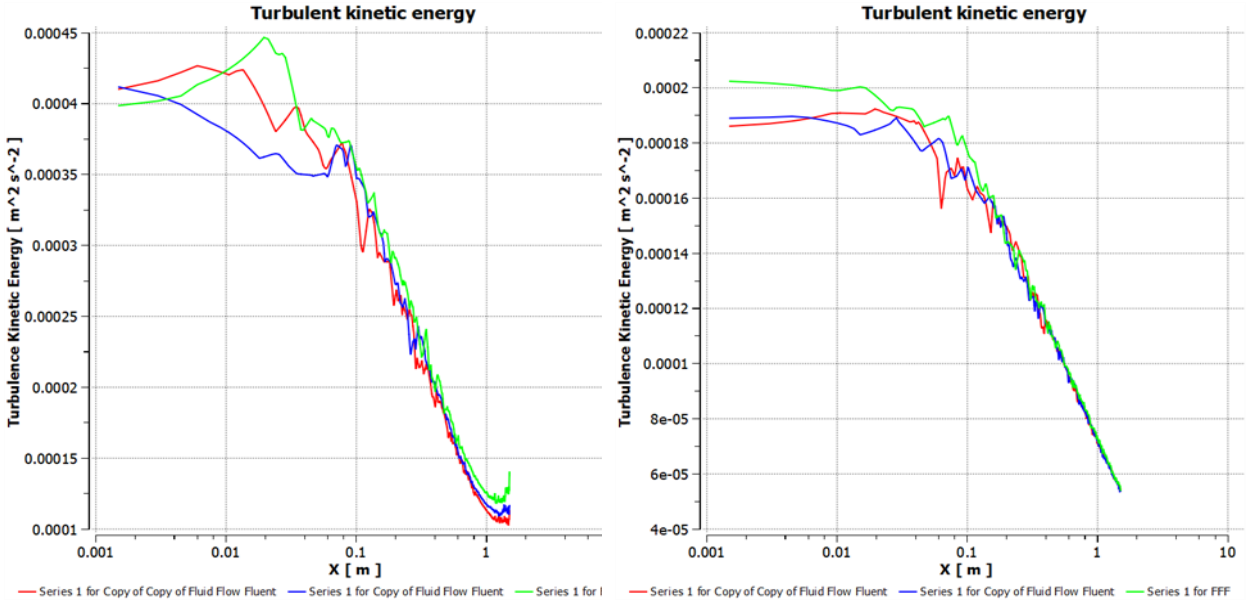

(a) (b)

Fig. 4. Graft quality of turbulence vs X (a) Diameter 0.01 m (b) Diameter 0.02 m

Looking at the pipe with a 0.1 m diameter at the first chart a, the pressure is already quite high just above 80 Pa right at the entrance (Figure 5). However, almost immediately it experiences a sharp and steep decline within the first 0.2 m of the pipe. This suggests significant resistance and energy loss as the fluid enters and starts to flow through the narrower space. While afterward, it continues to decline, it does so much milder and gentler as the fluid moves further downstream. By the time it reaches the end of the 1.6 m pipe, the pressure is nearly zero. It is likely that most of the pressure loss occurs right at the beginning, followed by stabilization as the flow continues. When it comes to the one with a 0.2 m diameter at the second chart b, it tells a similar but slightly different story.

Here, the pressure at the entrance is lower to begin with just above 65 Pa. It starts to decline steeply at the same first 0.2 mark but is not as sharp as in the narrower pipe. After that initial steep decline, it continues for a much longer length steadily, also approaching zero by the end of the pipe. It is clear from the two charts that the narrower pipe 0.1 m starts with a higher pressure at so the entrance, and loses it much quicker; while the wider pipe 0.2 m starts with a lower pressure and

experiences a less sharp drop. In both cases, most of the pressure loss is concentrated right at the beginning; the length of the pipe is characterized by slow, steady decline.

One can imagine it as water forced through two different straws one bigger and one thin. The narrow straw makes it difficult to go through initially, so the pressure drops rapidly as soon as it starts to flow in. The wider one is less restrictive, so while the pressure drop is still significant, it is not nearly as sharp. In both cases, however, once it starts flowing it flows smoothly, and pressure continues to drop slowly, steadily, until the fluid exits. These results once again demonstrate how pipe diameter affects pressure loss in internal flows: the narrower the pipe, the higher initial pressure and sharper drop with low downstream; and the wider it, the equation is the opposite due to a lack of restriction. This is extremely important when it comes to planning piping systems since they have to be designed to accommodate high-pressure systems.

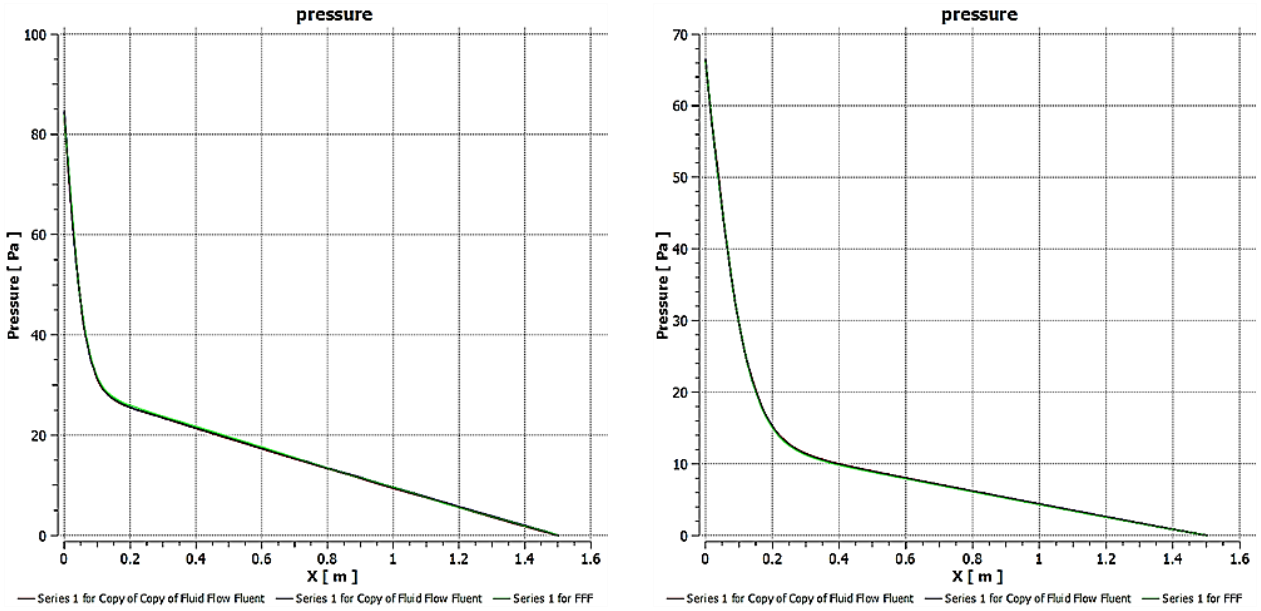

(a) (b)

Fig. 5. Graft quality of pressure vs x (a) Diameter 0.01 m (b) Diameter 0.02 m

3.2 Velocity

Figure 6(a) show the velocity distribution for a single configuration. The main offtake is nicely progressive from blue to green to yellow – presumably indicating that as the liquid enters, it does so more slowly, then accelerates as it continues downstream. This colour change at the branch reflects a change in velocity redistribution. One of the fluid streams slows as it moves into the branches, while the main leg still carries the fastest flow, denounced by the red streak. A similar pattern was seen for image Figure 6(b). However, with some slight differences (likely due to increased diameter or changes in flow conditions). The velocity in the main pipe continues to be high but you can see that the branches are working more with longer regions of green and yellow. This implies that, for a bigger diameter, the fluid can go at much higher speed when it is being divided, therefore the energy loses at the junction are lower.

Figure 6(c) restricts only to the 0.1 m diameter case. Here the story is clear: the main pipe is mostly red, which shows that the fluid is moving fastest along the centre line. Some of that energy is depleted as the flow approaches the Y-junction, and the fluid decelerates in the branches a tendency represented by the shift to green and blue. Such a pattern is common at junctions (local divergence), changing flow into a positive extra kinetic energy source and velocity reduction. As a

whole, these velocity contours visually show how the profile of the pipe and the junction affect the flow pattern. Max velocities are carried in the primary leg of the pipe, particularly the smaller pipe, while the secondary pipes slow down as the flow divides and changes direction. This becomes essential for the engineers so that they can be aware of where in the pipeline they could potentially face a problem such as erosion, pressure drop, flow separation and optimize the design of pipes that can efficiently transport the fluid.

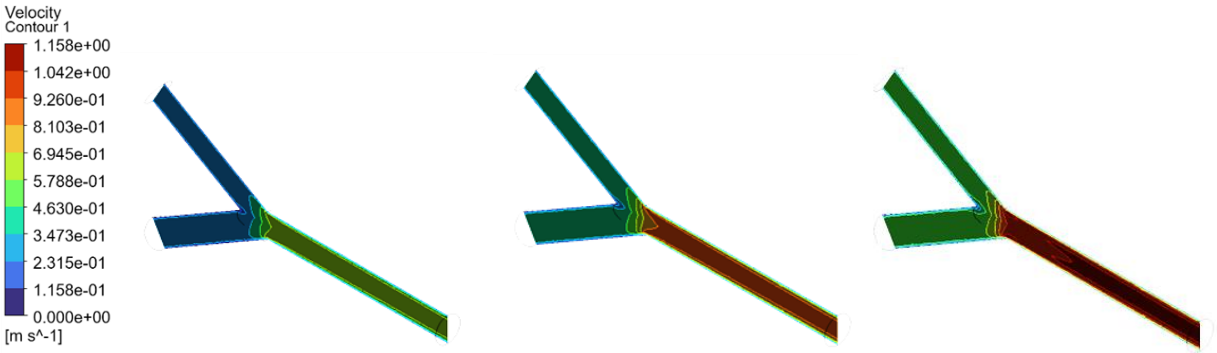

(a) (b) (c)

Fig. 6. Diameter 0.1 m

For Figures 7(a) to (c) represented the same Y-junction geometry but with different flow rates and/or chamber precipitate/simulation conditions. The colour scale on the left lets us judge the speed at which the fluid is moving: Deep blue shows places it is flowing quite slowly; bright red shows place the fluid is racing at its highest speed, up to a little over 1.26 meters a second. In Figure 7(a), one can observe that the incoming flow into the main pipe flows towards the junction. Velocity is moderate, mostly in greens and yellows, demonstrating a consistent but not very fast flow. The fluid slows down as it churns round the split, particularly amongst the branches, where it is a lovely blue and green. This means that the flow is losing energy as it bifurcates, and the branches are taking the fluid away at a more leisurely speed.

When we go to Figure 7(b), the story changes. In here, the main pipe also shows wider yellow and even some orange above it, signifying a faster fluid velocity than in (a). The velocity is still higher when the flow arrives and passes through the junction, and the branches look more green and yellow. In other words, in the case of some fronds, the fluid holds onto more of its speed as it splits, and the branches can transport a faster flow. Last but not least, Figure 7(c) shows the most spectacular case. "You've got this dominant bright red and orange over the main pipe, and that's the fluid clearly at work at its maximum speed yet. After the breakup, the branches still very fast, we know that because there are still yellow and green around. Flow here is unsolved for the most part, giving it plenty of energy and force as it splits at the fork.

These images in general demonstrate how different flow rate regime or PDMS simulation conditions can influence the distribution of velocities in the Y-junction. The bottom line is that, if you move the fluid faster through the main pipe (i.e. if you increase the driving force or thickness factor, or raise the inlet velocity), then this will translate into an increase in the speed of the fluid in the branches after the split. This information is important for engineers and designers, who can use it to estimate how different operating conditions will affect the performance and efficiency of pipe systems, particularly in complex geometries such as T-junctions where the flow can have unpredictable behaviour.

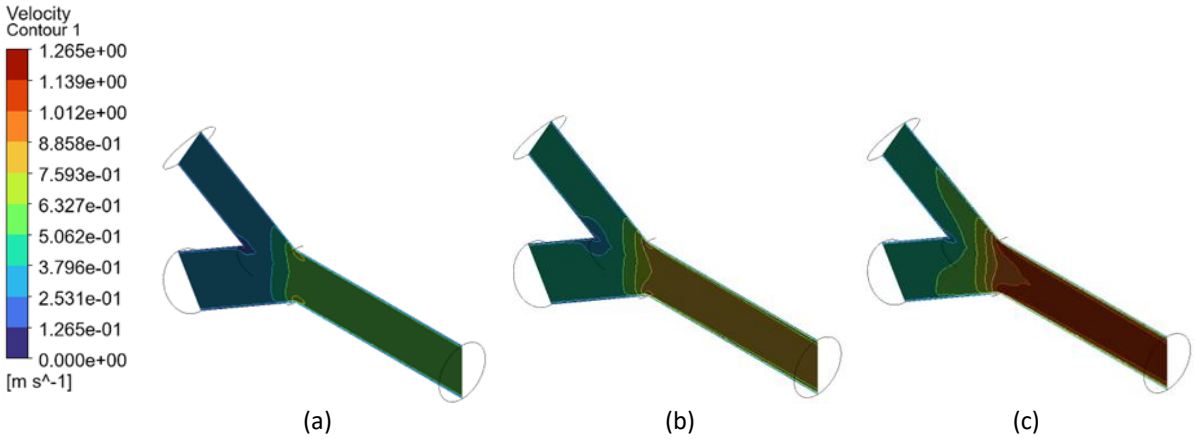

(a) (b) (c)

Fig. 7. Diameter 0.2 m

3.3 Turbulent Kinetic Energy

Based on Figure 8 the colours on each pipe, from deep blue to bright red, reflect the intensity of the turbulent kinetic energy, with blue representing the calmer regions and red showing the most energetic areas of turbulence. For Figure 8(a), the pipe is characterized by dark blue, meaning that the turbulent kinetic energy is quite low for most of this system. We can see a thin line of a lighter tone of colour around the pipe wall and branches, which indicates that there's a small region where there might be turbulence as well; however, it's hugging the wall and is incredibly weak. Whereas, the similar case except that the thin line around the pipe wall is a little bit more pronounced, and it continues further down the line inside the pipe than before (Figure 8(a)). This thinner line changes its colour slightly towards green and yellow, indicating that the turbulent kinetic energy is slightly higher than in Figure 8(a). This implies that under these conditions, this system is slightly more agitated, especially where the flow is affected by the pipe-wall interaction.

Finally, in Figure 8(c), the story is much clearer. We can see that the thin line near the pipe wall is developed, and it extends all the way both from the main inlet, through the junction, and into the branches. The line is much brighter around this image, as it gets to move towards yellow and even light orange shades. This indicates that the turbulent kinetic energy is higher, meaning that the fluid is under more chaotic, energetic flow conditions, especially where the flow is splitting in the Y-junction. In all three images, the core of the pipe remains dark blue, indicating that the flow is relatively calm but turbulent areas are present near the walls. This is typically the case with pipe flows since the walls generate the most turbulence due to the interaction and Y-junctions because the flow is encountering significant changes in direction.

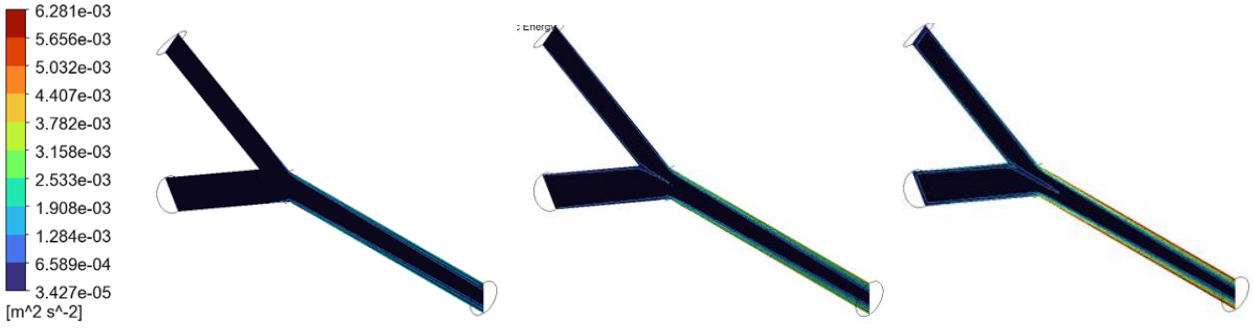

(a) (b) (c)

Fig. 8. Diameter 0.1 m

Subsequently, Figure 9(a) the setting depicts the beginning of the story as relatively undisturbed. Dark blue, corresponding to the smallest values of TKE on the colour scale, dominates the entire pipe. There is only an extremely thin pale line of slightly lighter blue tracking along the walls of the pipe, which indicates a certain degree of turbulence close the boundaries where the fluid slides past the circumference of the pipe. The central flow is calm; undisturbed. Besides, the thin boundary layer of turbulent flow along the pipe wall becomes more pronounced and coherent, extending over a longer part of the main pipe, and in fact into the branch pipes. The colour changes slightly toward green in some spots, indicating a mild overrun in turbulent kinetic energy (Figure 9(b)). This implies that under these conditions, the fluid is slightly more active near the sidewalls, in particular at the branching region of the Y-junction.

In Figure 9(c) the turbulence narrative climaxes. The wall-bounded turbulence streak now appears more prominent and stretches the length of the main pipe and both branches. The colours right along this boundary are brighter—towards the green and even yellow—indicating that the turbulent kinetic energy has gone up still further. What this is saying is that the fluid is moving around more "energetically" and more in a chaotic manner, especially at the junction / walls, while in the middle of the pipe: relatively calm there. In all three instances, one thing becomes apparent: the turbulence is primarily forced to the walls of the pipe and at the junction, but the centre of the pipe is calm and stays calm. This behaviour is often observed in piped flows, where turbulence is generated by the wall of the pipe and abrupt changes in direction at junctions.

In short, these results indicate that turbulence is low in the core but higher near the walls and particularly at the bifurcation in a Y-junction 0.2 m diameter pipe. This intensity of the turbulence increases from Figures 9(a) to (c), it is likely that such a phenomenon is due to changes in inflow conditions, or inlet velocity. For engineers and designers, this information is vital–it shows where mixing, wear or energy losses are more likely to be, leading to better design and maintenance of piping systems.

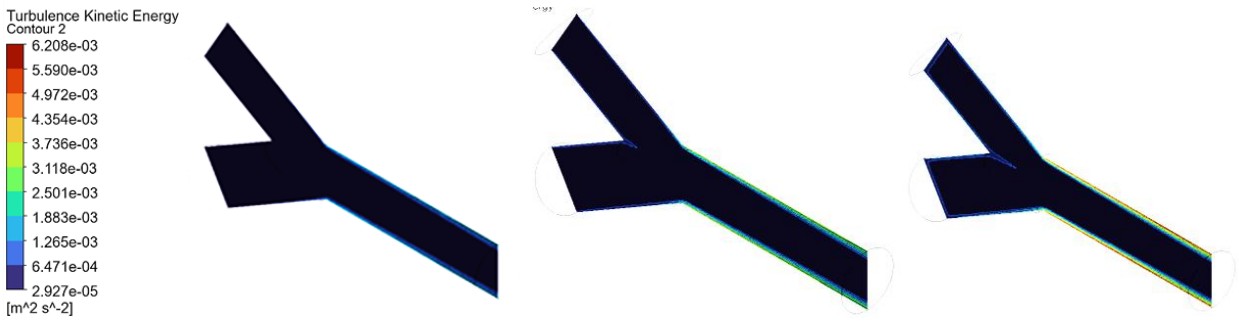

(a) (b) (c)

Fig. 9. Diameter 0.2 m

3.4 Pressure

The solution is presented in Figure 10 and shows the pressure distribution in a Y-shape pipe system with branch and main pipe diameters equal to 0.1 m. The pressure fluctuation is colour coded, in the colormap, the red stands for pressure as high as 519 Pa, while blue as low as -279 Pa. In each of the three sub-figures, referred as Figures 10(a) to 10(c), the highest pressure occurs at the bifurcation (the point where the pipe stems into two branches). This area is always depicted in red/oranges, which implies high-pressure accumulation at the bifurcation. As the flow from these points diverges between the branches, pressure diminishes incrementally. This is mapped from red

and orange at the intersection, to green and yellow, and finally to blue at the termini of the conduits, where the pressure is at its lowest.

Each subsection corresponds to a different choice or perspective, yet the general trend persists. This can be observed in Figure 10(a) where pressure distribution is smoother from high to low pressure values. In subfigure b, the region of high pressure covers a greater part of the branches, indicating a case with higher input pressure or under different flow conditions. Figure 10(c) presents a pattern similar to Figure 10(b), but the high-pressure region is not as far-reaching as in Figure 10(b), perhaps because of a different boundary condition or flow rate. On the whole, such findings directly show where the pressure flows in the configuration of branching pipe system. The greatest pressures are at the bifurcation at which the flow separates and the pressure diminishes as the fluid flows along the branches. This behaviour is to be expected for such systems, and it is of particular networking-interest to know where reinforcements in the network should be made and how the fluid will act as it moves through the network.

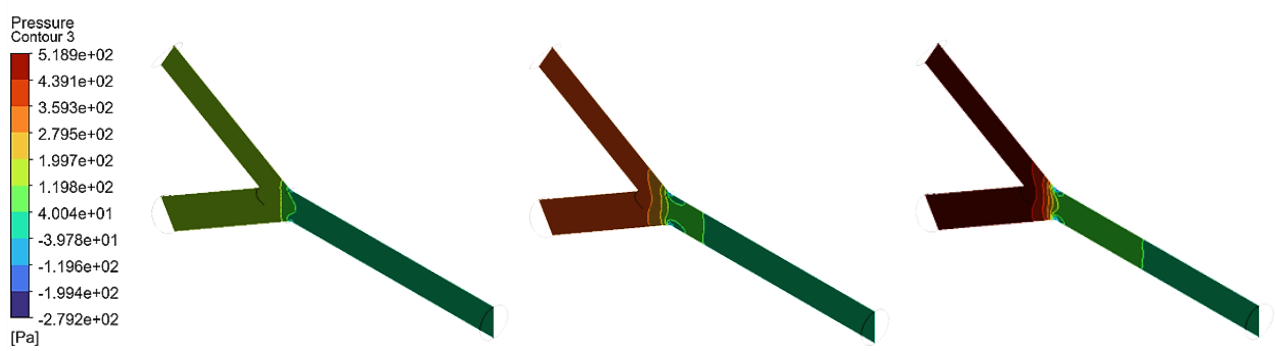

(a) (b) (c)

Fig. 10. Diameter 0.1 m

Figure 11 show pressure distribution in a Y-type pipe system with each pipe diameter equal to 0.2 m. The colour map along the left side of the figure varies from dark blue (minimum pressure, -541 Pa) to light red (maximum pressure, 481 Pa). In the three subfigures, the maximum pressure is located at the connection point of original pipe of two branches. This region is based in red and orange indicating that high pressure values are concentrated in the area of the bifurcation. As fluid leaves the junction and passes through the branches and main pipe, pressure continues to increase. This is evidenced by the colour shift from red, to orange near the junction, and green, and finally blue toward the exits in the pipes. The pressure loss is the same for all the subfigures, but at the same time the high-pressure region's area and strength is a little bit different

For Figure 11(a), the high-pressure region is fairly localized at the junction and with moderate smooth drop of pressure on waves propagating along the branches. Figure 11(b) provides a larger area of high pressure which is suggestive of a case of a higher inlet pressure or a change in the flow regime. Figure 11(c) also shows that there is a large high-pressure region at the junction with pressure gradient reaching up further down the main pipe and branches in comparison to Figure 11(a). In general, the results demonstrate the greatest pressure is developed at the bifurcation, followed by a decay and redistribution in the network pipe line. It is a common pattern in branching pipe system and is useful in describing where structural support may be necessary and the behaviour of the fluid flow through the system. Colour contours improve the visualization of such pressure variations, and help in the evaluation and design of these piping networks.

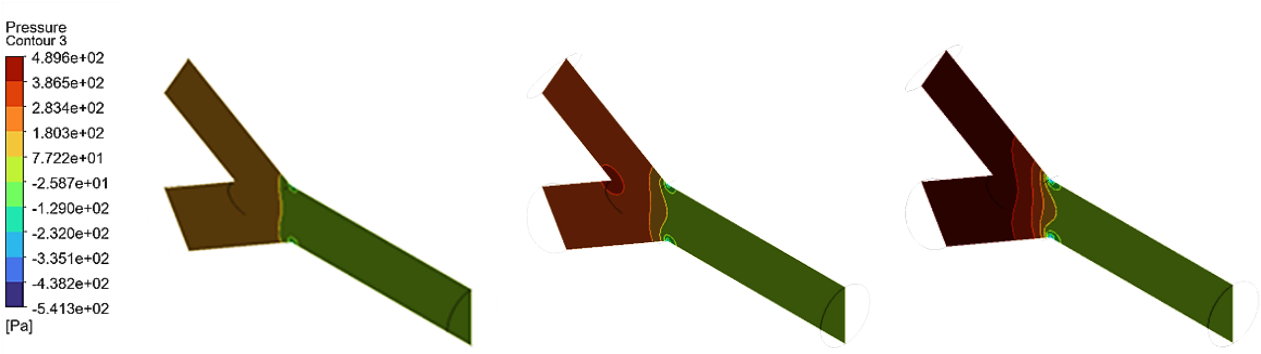

(a) (b) (c)

Fig. 11. Diameter 0.2 m

4. Conclusions

Based on the CFD simulation of the Y-shaped pipeline with two different diameters (0.1 m and 0.2 m), it can be concluded that the pipe diameter has a significant effect on the fluid flow characteristics, namely velocity, turbulence kinetic energy, and pressure distribution. For velocity, the results show that smaller diameter pipes (0.1 m) generate higher flow speeds, especially around the junction and outlet. This is due to the reduced cross-sectional area, which forces the fluid to accelerate. In contrast, the 0.2 m pipe allows for a slower and more uniform velocity profile due to the larger flow area, reducing the overall velocity magnitude. In terms of turbulence, the 0.1 m diameter pipe exhibited higher turbulence kinetic energy, particularly at the Y-junction, indicating more chaotic and unstable flow behaviours. This is a result of sharper flow redirection in the narrower pipe. The 0.2 m pipe, on the other hand, demonstrated lower turbulence levels, reflecting more stable and smoother fluid motion throughout the pipeline.

Pressure analysis revealed that pressure drops are more significant in the 0.1 m pipe, where a sharp decrease in pressure occurs along the flow direction due to higher velocity and turbulence. Meanwhile, the 0.2 m pipe experienced a more gradual and consistent pressure drop, maintaining more stable pressure throughout the pipeline. In conclusion, increasing the pipeline diameter results in a reduction of flow velocity and turbulence, as well as a more stable pressure distribution. Therefore, for applications requiring stable flow with minimal energy loss and turbulence, a larger diameter Y-pipeline is preferable. However, if higher velocity is desired for specific fluid dynamics, a smaller diameter may be more suitable though with the trade-off of increased turbulence and pressure drop.

References

[1] Gajbhiye, Bhavesh D., Harshawardhan A. Kulkarni, Shashank S. Tiwari, and Channamallikarjun S. Mathpati. "Teaching turbulent flow through pipe fittings using computational fluid dynamics approach." *Engineering Reports* 2, no. 1 (2020): e12093. https://doi.org/10.1002/eng2.12093

[2] Miyazaki, Shohei, Keiichi Itatani, Toyoki Furusawa, Teruyasu Nishino, Masataka Sugiyama, Yasuo Takehara, and Satoshi Yasukochi. "Validation of numerical simulation methods in aortic arch using 4D Flow MRI." *Heart and Vessels* 32, no. 8 (2017): 1032-1044. https://doi.org/10.1007/s00380-017-0979-2

[3] Taha, Enas Salman, Mohammed A. Abdulwahid, Akeel M. Ali Morad, and Qusay A. Maatooq. "Computational fluid dynamic analysis of the flow through T-junction and venturi meter." *IMDC-IST* (2022). https://doi.org/10.4108/eai.7-9-2021.2314880

[4] Doi, Taiga, Takashi Futatsugi, Michio Murase, Kosuke Hayashi, Shigeo Hosokawa, and Akio Tomiyama. "Countercurrent Flow Limitation at the Junction between the Surge Line and the Pressurizer of a PWR." *Science and Technology of Nuclear Installations* 2012, no. 1 (2012): 754724. https://doi.org/10.1155/2012/754724

[5] Marušić-Paloka, Eduard. "Rigorous justification of the Kirchhoff law for junction of thin pipes filled with viscous fluid." *Asymptotic Analysis* 33, no. 1 (2003): 51-66. https://doi.org/10.3233/ASY-2003-543

[6] Ando, Toshitake, Toshihiko Shakouchi, Satoru Takamura, and Koichi Tsujimoto. "Effects of flow rate ratio on loss reduction of T-junction pipe." *Journal of Fluid Science and Technology* 9, no. 3 (2014): JFST0045-JFST0045.
[7] Mohammadi M. and M. Rahimi, "Numerical investigation of turbulent flow in a Y-shaped pipe," *Journal of Mechanical Science and Technology* 27, no. 11 (2013): 3523-3531.
[8] Li, Xiaoyu, Geyu Shen, Ping Liu, Jinchen Gao, Ningxin Gu, and Zhaoming Meng. "The Effect of Different Branch Angles and Different Branch Pipe Sizes on the Onset Law of Liquid Entrainment." *Frontiers in Energy Research* 8 (2020): 95. https://doi.org/10.1016/j.cherd.2020.01.006
[9] Vigolo, Daniele, Stefan Radl, and Howard A. Stone. "Unexpected trapping of particles at a T junction." *Proceedings of the National Academy of Sciences* 111, no. 13 (2014): 4770-4775. https://doi.org/10.1073/pnas.1321585111
[10] Lučin, Ivana, Lado Kranjčević, Zoran Čarija, and Antonio Mogorović. "Experimental Setup of Fluid Mixing in Double Tee-Junctions." In *Annals of DAAAM and Proceedings of the International DAAAM Symposium*, pp. 1059-1064. Beč: DAAAM International Vienna, 2018. https://doi.org/10.2507/29th.daaam.proceedings.151
[11] Hoi, Yiemeng, Scott H. Woodward, Minsuok Kim, Dale B. Taulbee, and Hui Meng. "Validation of CFD simulations of cerebral aneurysms with implication of geometric variations." *Journal of Biomechanical Engineering* 128 no. 6 (2006): 844-851. https://doi.org/10.1115/1.2354209
[12] Ferreira, Ronaldo Novaes, Leonardo Machado Da Rosa, and Johannes Gérson Janzen. "Effect of 90° elbows on pump inlet flow conditions." *Applied Water Science* 10, no. 7 (2020): 1-8. https://doi.org/10.1007/s13201-020-01255-7
[13] Decaix, Jean, Jean-Louis Drommi, François Avellan, and Cécile Münch-Alligné. "CFD simulations of hydraulic short-circuits in junctions, application to the Grand'Maison power plant." In *IOP Conference Series: Earth and Environmental Science*, vol. 1079, no. 1, p. 012106. IOP Publishing, 2022. https://doi.org/10.1088/1755-1315/1079/1/012106
[14] Decaix, Jean, Mathieu Mettille, Nicolas Hugo, Bernard Valluy, and Cécile Münch-Alligné. "CFD investigation of the hydraulic short-circuit mode in the FMHL/FMHL+ pumped storage power plant." *Energies* 17, no. 2 (2024): 473. https://doi.org/10.3390/en17020473
[15] Yousef, Khaled, Ahmed Hegazy, and Fatma Saleh. "Numerical Study of Induced Condensation upon Mixing Flows of Water-stream Flow in a Tee-Junction Pipe." *ERJ. Engineering Research Journal* 44, no. 2 (2021): 159-174. https://doi.org/10.21608/erjm.2021.52289.1056
[16] Lintermann, Andreas. "Computational meshing for CFD simulations." In *Clinical and biomedical engineering in the human nose: A computational fluid dynamics approach*, pp. 85-115. Singapore: Springer Singapore, 2020. https://doi.org/10.1007/978-981-15-6716-2_6
[17] Lopez-Santana, Gabriela Belen, Andrew Kennaugh, and Amir Keshmiri. "Experimental techniques against RANS method in a fully-developed turbulent pipe flow." (2021). https://doi.org/10.3390/fluids7020078
[18] Zhu, Na, Pingfang Hu, Yu Lei, Zhangning Jiang, and Fei Lei. "Numerical study on ground source heat pump integrated with phase change material cooling storage system in office building." *Applied Thermal Engineering* 87 (2015): 615-623. https://doi.org/10.1016/j.applthermaleng.2015.05.056
[19] Raschi, Marcelo, Fernando Mut, Greg Byrne, Christopher M. Putman, Satoshi Tateshima, Fernando Viñuela, Tetsuya Tanoue, Kazuo Tanishita, and Juan R. Cebral. "CFD and PIV analysis of hemodynamics in a growing intracranial aneurysm." *International Journal for Numerical Methods in Biomedical Engineering* 28, no. 2 (2012): 214-228. https://doi.org/10.1002/cnm.1459
[20] Chen, L. Y., L. X. Zhang, and X. M. Shao. "The motion of small bubble in the ideal vortex flow." *Procedia Engineering* 126 (2015): 228-231. https://doi.org/10.1016/j.proeng.2015.11.229